BASIC RESEARCH www.jasn.org

Protein Kinase G Inhibits Flow-Induced Ca^{2+} Entry into Collecting Duct Cells

Juan Du,*†‡ Wei-Yan Wong,*† Lei Sun,*† Yu Huang,*† and Xiaoqiang Yao*†

*School of Biomedical Sciences and †Li Ka Shing Institute of Health Sciences, Chinese University of Hong Kong, Hong Kong, China; and ‡Department of Physiology, Anhui Medical University, He Fei, China

ABSTRACT

The renal cortical collecting duct (CCD) contributes to the maintenance of K^+ homeostasis by modulating renal K^+ secretion. Cytosolic Ca^{2+} ($[Ca^{2+}]_i$) mediates flow-induced K^+ secretion in the CCD, but the mechanisms regulating flow-induced Ca^{2+} entry into renal epithelial cells are not well understood. Here, we found that atrial natriuretic peptide, nitric oxide, and cyclic guanosine monophosphate (cGMP) act through protein kinase G (PKG) to inhibit flow-induced increases in $[Ca^{2+}]_i$ in M1-CCD cells. Coimmunoprecipitation, double immunostaining, and functional studies identified heteromeric TRPV4-P2 channels as the mediators of flow-induced Ca^{2+} entry into M1-CCD cells and HEK293 cells that were coexpressed with both TRPV4 and TRPP2. In these HEK293 cells, introducing point mutations at two putative PKG phosphorylation sites on TRPP2 abolished the ability of cGMP to inhibit flow-induced Ca^{2+} entry. In addition, treating M1-CCD cells with fusion peptides that compete with the endogenous PKG phosphorylation sites on TRPP2 also abolished the cGMP-mediated inhibition of the flow-induced Ca^{2+} entry. Taken together, these data suggest that heteromeric TRPV4-P2 channels mediate the flow-induced entry of Ca^{2+} into collecting duct cells. Furthermore, substances such as atrial natriuretic peptide and nitric oxide, which increase cGMP, abrogate flow-induced Ca^{2+} entry through PKG-mediated inhibition of these channels.

J Am Soc Nephrol 23: 1172–1180, 2012. doi: 10.1681/ASN.2011100972

The cortical collecting duct (CCD) is an important renal tubular segment that has final control over renal K^+ secretion.[1] The magnitude of K^+ secretion in the CCD is partially determined by the electrochemical gradient generated by transepithelial Na^+ absorption that favors K^+ diffusion from the cells into the tubular fluid.[2,3] Ion transport in the CCD, including K^+ secretion (and Na^+ absorption), is regulated by chemical factors that include hormones and autocrines in addition to physical factors such as tubular fluid flow. Atrial natriuretic peptide and nitric oxide are two important chemical factors that inhibit K^+ secretion and Na^+ absorption in the CCD.[4,5] However, high tubular flow stimulates K^+ secretion in the CCD.[2,6]

An important early signal for flow response is the rise of cytosolic Ca^{2+} ($[Ca^{2+}]_i$) in CCD epithelial cells. Evidence suggests that these $[Ca^{2+}]_i$ rises are requisite for flow-induced K^+ secretion in these cells.[2,6] There is intense interest in searching for the plasma membrane channels that mediate flow-induced Ca^{2+} entry in renal epithelial cells. Several candidate channels have been proposed, including transient receptor potential vanilloid 4 (TRPV4),[7,8] transient receptor potential polycystin 1 (TRPP1)-TRPP2 complex,[9] and heteromeric TRPV4-P2 channels.[10] It is suggested that TRPP1 and TRPP2 may form a physical complex in which TRPP1 serves as a sensor to transduce the flow stimuli to TRPP2, which is a Ca^{2+} entry channel.[9] A study by Köttgen *et al.*[10] showed that, in Madin–Darby canine kidney distal tubule cells, TRPV4 and TRPP2 formed heteromeric TRPV4-P2 channels in the cilia, which is a crucial structure for flow sensation.[9] The study by Köttgen *et al.*[10] also suggested that the heteromeric TRPV4-P2 channels mediate flow-induced Ca^{2+} entry in these cells.

Received October 8, 2011. Accepted February 15, 2012.

Published online ahead of print. Publication date available at www.jasn.org.

Correspondence: Dr. Xiaoqiang Yao, School of Biomedical Sciences, Chinese University of Hong Kong, Hong Kong, China. Email: yao2068@cuhk.edu.hk

More recently, we found that additional heteromeric TRP channels, namely TRPV4-C1 channels, are responsible for flow-induced Ca^{2+} entry in vascular endothelial cells.[11]

Very little is known about the regulation of flow-induced Ca^{2+} entry in renal epithelial cells. TRPV4 is activated by hypotonic cell swelling.[12] The activation of TRPV4 by cell swelling is reportedly mediated through arachidonic acid and its downstream metabolite epoxyeicosatrienoic acids.[12] The flow activation of TRPV4 in ciliated oviductal cells is also believed to be mediated by arachidonic acid.[13] In addition, a number of other signaling molecules/pathways, including protein kinase C, EGFs, and receptor tyrosine kinases, may regulate TRPV4 and/or TRPP2,[12,14] but it is unclear whether these molecules/pathways play any role in flow-induced Ca^{2+} responses.

The present study identified heteromeric TRPV4-P2 as the channels that mediate the flow-induced Ca^{2+} entry in M1-CCD cells. More importantly, we uncovered a novel regulatory mechanism for this Ca^{2+} entry. We found that cyclic guanosine monophosphate (cGMP) and protein kinase G (PKG) inhibit the Ca^{2+} entry through their action on heteromeric TRPV4-P2 channels. PKG phosphorylates on $TRPP2^{T719A}$ and $TRPP2^{S827A}$ to inhibit heteromeric TRPV4-P2 channels, thereby negatively regulating the flow-induced Ca^{2+} entry in M1-CCD cells.

RESULTS

Effect of cGMP, PKG, Atrial Natriuretic Peptide, and Nitric Oxide on Flow-Induced Ca^{2+} Entry in M1-CCD cells

The application of fluid flow induced $[Ca^{2+}]_i$ transients in M1-CCD cells (Figure 1, A and B). The Ca^{2+} transients were absent when the bath solution was Ca^{2+}-free (Figure 1B), suggesting the involvement of Ca^{2+} entry but not store Ca^{2+} release. In the presence of 8-Br-cGMP (2 mM), which activates PKG, flow-induced $[Ca^{2+}]_i$ transients were inhibited (Figure 1, A and B). KT5823 (1 μM), a selective inhibitor of PKG,[15] reversed the inhibitory action of 8-Br-cGMP (Figure 1, A and B). KT5823 treatment also made the flow-induced $[Ca^{2+}]_i$ transients much more sustained. After the $[Ca^{2+}]_i$ reached its plateau, the removal of bath Ca^{2+} caused an immediate reduction in the $[Ca^{2+}]_i$ level (Supplemental Figure 1), further supporting the involvement of Ca^{2+} entry but not store Ca^{2+} release for the $[Ca^{2+}]_i$ rises. These data showed the inhibitory effect of cGMP and PKG on flow-induced Ca^{2+} entry in M1-CCD cells.

Atrial natriuretic peptide and nitric oxide are two endogenous factors that increase the cytosolic cGMP level in renal CCD cells.[4,5] As expected, both atrial natriuretic peptide (10 nM) and a nitric oxide donor (+/−)-S-nitroso-N-acetylpenicillamine (SNAP; 50 μM) inhibited the flow-induced Ca^{2+} entry in M1-CCD cells (Figure 1, C and D). This inhibition was reversed by KT5823 (1 μM), suggesting the involvement of PKG (Figure 1, C and D). Note that a tiny residual fluorescence change to flow was observed in cGMP-treated M1-CCD cells (Figure 1A), nontreated wild-type HEK293 cells (data not shown), and empty plasmid vector-transfected HEK293 cells (see Figure 3). This fluorescence change may reflect a slight cell movement during flow disturbance, or it may be caused by residual flow-sensitive components.

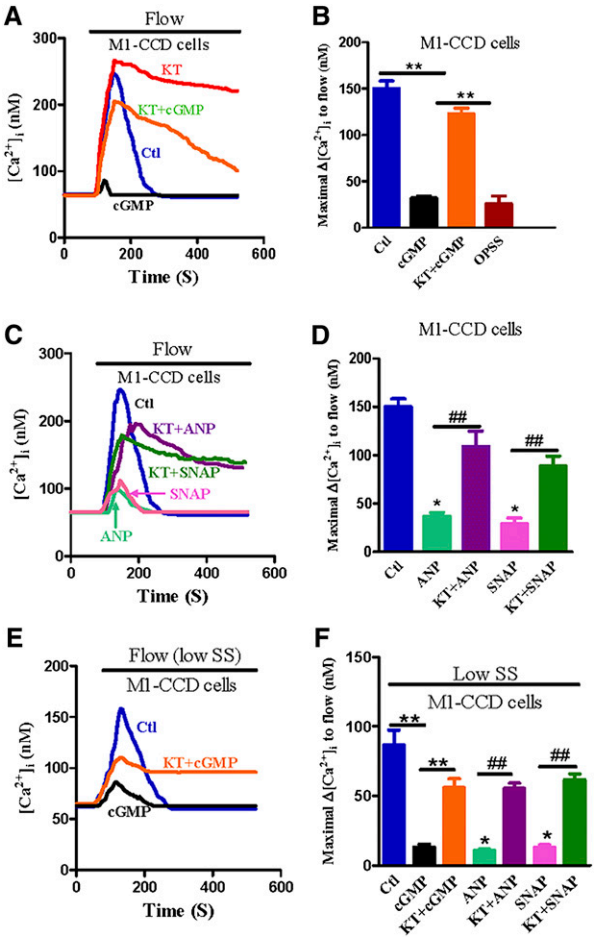

Figure 1. Effect of cGMP, PKG, atrial natriuretic peptide, and nitric oxide on flow-induced Ca^{2+} entry in M1-CCD cells. (A, C, and E) Representative traces illustrating the time course of flow-induced $[Ca^{2+}]_i$ responses at a shear stress of (A and C) 5 dyne/cm^2 or (E) 0.5 dyne/cm^2 (low saline solution [SS]). (B, D, and F) Summary showing the maximal change in flow-induced $[Ca^{2+}]_i$ responses ($\Delta[Ca^{2+}]_i$) for cells at a shear stress of (B and D) 5 dyne/cm^2 or (F) 0.5 dyne/cm^2 (low SS). Cells were pretreated for 10 minutes with (A, B, E, and F) 2 mM 8-Br-cGMP with or without 1 μM KT5823, (C, D, and F) 10 nM atrial natriuretic peptide (ANP) with or without 1 μM KT5823, or (C, D, and F) 50 μM SNAP with or without 1 μM KT5823. Control had no treatment. Cells were bathed in NPSS containing 1% BSA except for 0PSS series (a bar in B), in which the bath was Ca^{2+}-free. The solid bar on top of the traces indicates the period when laminar flow was applied. Data are given as the mean ± SE (n=8–10 experiments and 10–20 cells per experiment). **P<0.01 versus 8-Br-cGMP (B and F). *P<0.01 versus control (D and F). $^{\#\#}P$<0.01 versus the corresponding ones without KT5823. OPSS, Ca^{2+}-free physiological saline solution.

The above-mentioned experiments were performed under a flow shear force of ~5 dyne/cm^2. We also tested a flow shear force of 0.5 dyne/cm^2, which is the physiologic shear force for distal tubular cells expected in an euvolemic animal.[16] The flow at 0.5 dyne/cm^2 elicited similar $[Ca^{2+}]_i$ rises but at a smaller magnitude (Figure 1, E and F). The $[Ca^{2+}]_i$ rises were, again, sensitive to the inhibition of 8-Br-cGMP (2 mM), atrial natriuretic peptide (10 nM), and SNAP (Figure 1, E and F). KT5823 (1 μM) reversed the inhibition (Figure 1, E and F). Because the magnitudes of $[Ca^{2+}]_i$ rises at ~5 dyne/cm^2 were relatively large, the data were easy to analyze and subjected to less error. Therefore, ~5 dyne/cm^2 was used in the latter experiments.

Role of TRPV4, TRPP2, and Transient Receptor Potential Canonical 1 in Flow-Induced Ca^{2+} Entry in M1-CCD Cells

Dominant negative constructs for TRPV4 and TRPP2 (TRPV4^{M680D} and TRPP2^{D511V}, respectively) were used to explore the possible roles of TRPV4 and TRPP2 in the flow-induced Ca^{2+} entry in M1-CCD cells.[17,18] The expressions of TRPV4^{M680D} and TRPP2^{D511V} each abolished the flow-induced Ca^{2+} entry in these cells (Figure 2, A and B). The possible involvement of transient receptor potential canonical 1 (TRPC1) was also explored using a TRPC1-blocking antibody T1E3. T1E3 targets the E3 region near the ion permeation pore of TRPC1.[19,20] The specificity of T1E3 was previously confirmed in immunoblots and functional studies.[11,19,20] The immunostaining of nonpermeabilized HEK293 cells that were overexpressed with TRPV4 and TRPC1 showed that T1E3 staining was concentrated at the plasma membrane (Supplemental Figure 2), supporting that T1E3 binds to the extracellular epitope of TRPC1. Interestingly, the T1E3 treatment (1:100 for 1 hour) had no effect on the flow-induced Ca^{2+} entry in M1-CCD cells (Figure 2, C and D).

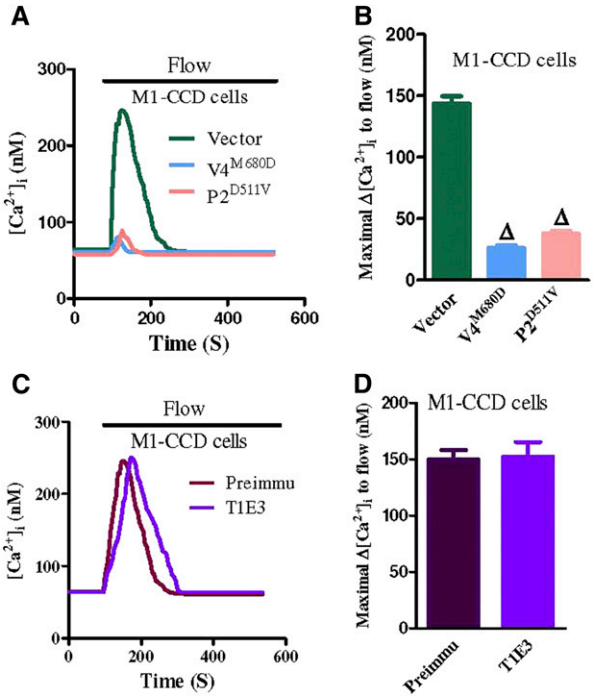

Figure 2. TRPV4 and TRPP2 involvement in flow-induced $[Ca^{2+}]_i$ entry in M1-CCD cells. (A and C) Representative traces illustrating the time course of flow-induced $[Ca^{2+}]_i$ responses. (B and D) Summary showing the maximal change in flow-induced $[Ca^{2+}]_i$ responses ($\Delta[Ca^{2+}]_i$). In A and B, the cells were transfected with an empty plasmid vector (vector), TRPV4^{M680D} (V4^{M680D}), or TRPP2^{D511V} (P2^{D511V}). In C and D, the cells were pretreated with Preimmune IgG (Preimmu) or T1E3. Data are given as the mean ± SE (n=8–10 experiments and 10–20 cells per experiment). $^{\Delta}P<0.01$ versus vector.

Physical Association of TRPV4 with TRPP2 in M1-CCD Cells

Coimmunoprecipitation and double immunostaining were used to explore the physical interaction of TRPV4 and TRPP2. Two antibodies for coimmunoprecipitation, the anti-TRPV4 antibody and anti-TRPP2 antibody, were previously reported to be highly specific.[21,22] In coimmunoprecipitation experiments, the anti-TRPP2 antibody could pull down TRPV4 in protein lysates freshly prepared from M1-CCD cells (Figure 3A). Furthermore, an anti-TRPV4 antibody could reciprocally pull down TRPP2 (Figure 3B). In control experiments in which the immunoprecipitation was performed with IgG purified from preimmune serum, no band was observed (Figure 3, A and B). These data indicate that TRPV4 physically associates with TRPP2 in M1-CCD cells.

The selective interaction of TRPV4 with TRPP2 was supported by double immunostaining. Staining for TRPV4 and TRPP2 was observed in cultured M1-CCD cells (Figure 3C). Overlaying the TRPV4 signal (green) with the signal of the TRPP2 (red) showed clear colocalization (yellow) of TRPV4 and TRPP2 (Figure 3, C–C″) in the cytosol and the plasma membrane. TRPV4 and TRPP2 were also found to be concentrated in the cilia in M1-CCD cells (Figure 3, D–D″).

Heteromeric TRPV4-P2 Channels and Their Role in the Flow-Induced Ca^{2+} Entry in HEK293 Cells That Were Overexpressed with TRPV4 and TRPP2

Attempts were made to verify whether TRPV4 and TRPP2 could interact with each other to form a flow-sensitive channel by overexpressing these two proteins in HEK293 cells. As Figure 4, A and B shows, the flow was able to induce $[Ca^{2+}]_i$ rises in HEK293 cells that were coexpressed with TRPV4 and TRPP2. The kinetics of $[Ca^{2+}]_i$ rises in these cells were different from the cells that were expressed with TRPV4 alone. For the former, the $[Ca^{2+}]_i$ responses to flow were sustained without apparent decay in the experimental duration of ~10 minutes (Figure 4A). For the latter, the responses to flow were transient (Figure 4A). In cells that were coexpressed with TRPV4 and TRPP2, the replacement of TRPV4 and TRPP2 with their mutant counterparts (TRPV4^{M680D} and TRPP2^{D511V}, respectively) each abolished the flow-induced $[Ca^{2+}]_i$ responses (Figure 4B). These data support the formation of heteromeric

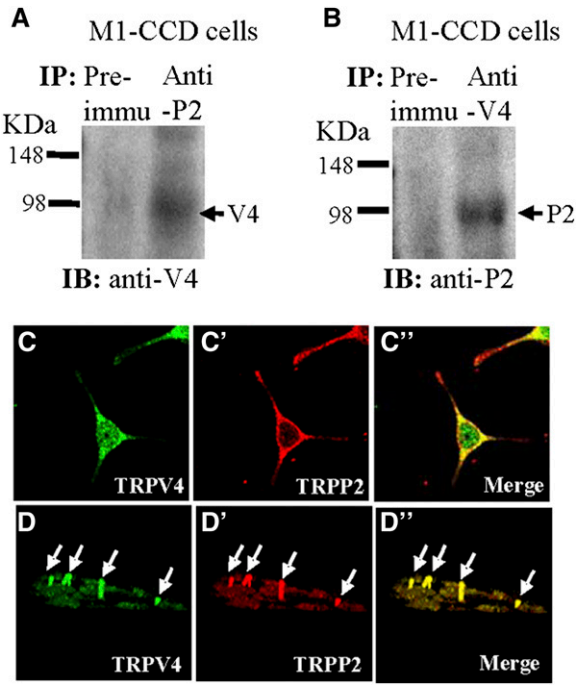

Figure 3. Physical interaction between TRPV4 and TRPP2 in M1-CCD cells. (A and B) Coimmunoprecipitation. The pulling antibody and the blotting antibody are indicated. Control immunoprecipitation was performed using preimmune IgG (labeled as Preimmu). Anti-P2 indicates anti-TRPP2, anti-V4 indicates anti-TRPV4, IB indicates immunoblot, and IP indicates immunoprecipitation (n=3 experiments). (C–D″) Double immunostaining. (C and D) TRPV4 and (C′ and D′) TRPP2 were colocalized in (C″ and D″; merge) the cytosol, the plasma membrane, and the primary cilium of M1-CCD cells. D–D″ are confocal images of z-series stacks showing the primary cilium emerging from the apical membrane.

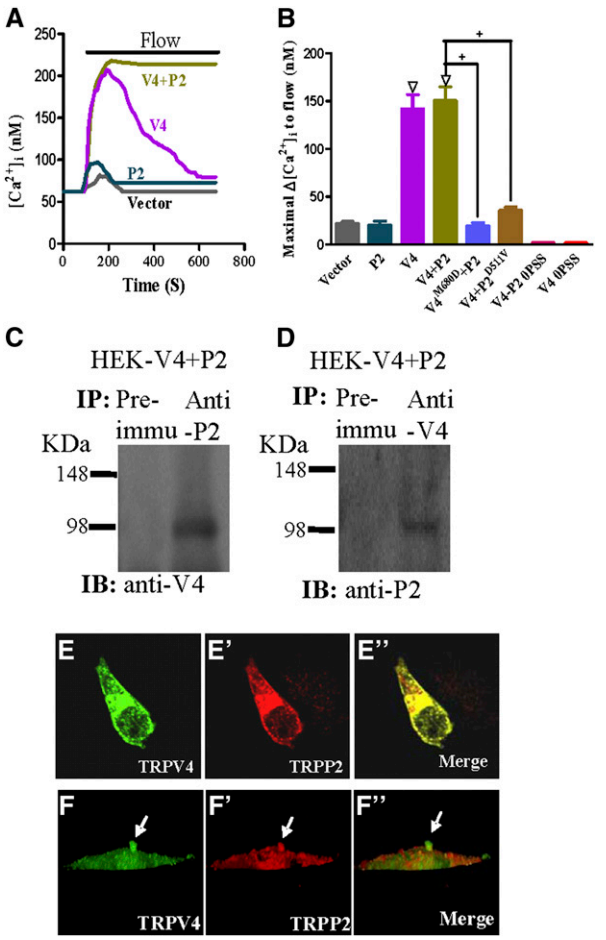

Figure 4. Physical association and functional role of TRPV4 and TRPP2 in HEK293 cells that were coexpressed with TRPV4 and TRPP2. (A and B) Flow-induced $[Ca^{2+}]_i$ responses. (A) Representative traces illustrating the time course of flow-induced $[Ca^{2+}]_i$ responses. (B) Summary showing the maximal change in flow-induced $[Ca^{2+}]_i$ responses ($\Delta[Ca^{2+}]_i$). Cells were bathed in NPSS containing 1% BSA except for 0PSS series (labeled bars in B), in which the bath was Ca^{2+}-free. Cells were transfected with an empty vector (vector), TRPP2 (P2), TRPV4 (V4), TRPV4+TRPP2 (V4+P2), $TRPV4^{M680D}$+TRPP2 ($V4^{M680D}$+P2), or TRPV4+$TRPP2^{D511V}$ ($V4+P2^{D511V}$). Data are given as the mean ± SE (n=6–8 experiments and 8–20 cells per experiment). $^{\Delta}P<0.01$ versus vector. $^{+}P<0.01$ versus V4+P2. (C and D) Coimmunoprecipitation. The pulling antibody and the blotting antibody are indicated. Control immunoprecipitation was performed using the preimmune IgG (Preimmu; n=3 experiments). (E–F″) Double immunostaining. (E and F) TRPV4 and (E′ and F′) TRPP2 were colocalized in (E″ and F″; merge) the cytosol, the plasma membrane, and the primary cilium of transfected HEK293 cells. F–F″ are confocal images of z-series stacks showing the primary cilium emerging from the apical membrane.

TRPV4-P2 channels and their functional role in mediating the flow-induced Ca^{2+} entry. In control experiments, vector-transfected HEK293 cells did not respond to flow (Figure 4, A and B). The flow also failed to elicit any $[Ca^{2+}]_i$ rise in HEK293 cells that were expressed with TRPP2 alone (Figure 4, A and B) or those cells that were coexpressed with TRPV4 and TRPP2 but bathed in a Ca^{2+}-free solution (Figure 4B).

Coimmunoprecipitation experiments found that TRPV4 and TRPP2 could pull each other down when they were coexpressed in HEK293 cells (Figure 4, C and D). Double immunostaining showed that TRPV4 and TRPP2 were colocalized in the cytosols and the plasma membrane of these cells (Figure 4, E–E″). Furthermore, TRPV4 and TRPP2 were found to be concentrated in the cilia (Figure 4, F–F″).

cGMP and PKG Regulation of the Flow-Induced Ca^{2+} Entry in HEK293 Cells That Were Overexpressed with TRPV4 and TRPP2

We next used the HEK293 cell overexpression system to confirm the PKG regulation of heteromeric TRPV4-P2 channels. In these experiments, HEK293 cells were first stably transfected with PKG1α and named PHEK cells. These PHEK cells expressed a much higher level of PKG1α compared with wild-type HEK293 cells.[23] The PHEK cells were then transiently transfected with either TRPV4 or TRPV4+TRPP2. In PHEK cells expressing TRPV4, the 8-Br-cGMP (2 mM) treatment had no effect on flow-induced $[Ca^{2+}]_i$ rises (Figure 5,

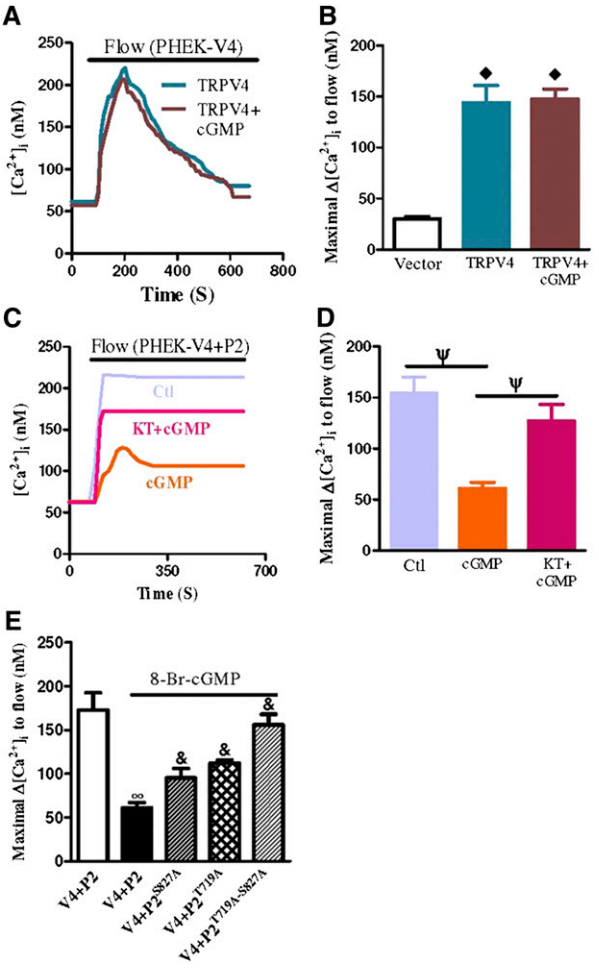

Figure 5. Flow-induced $[Ca^{2+}]_i$ responses in HEK293 cells that were transfected with individual TRPV4 or TRPP2 or cotransfected with both TRP isoforms. (A and C) Representative traces illustrating the time course of flow-induced $[Ca^{2+}]_i$ responses. (B, D, and E) Summary showing the maximal change in flow-induced $[Ca^{2+}]_i$ responses. HEK293 cells stably transfected with a PKG1α gene are labeled as PHEK cells. All cells were bathed in NPSS containing 1% BSA. Cells were pretreated with 8-Br-cGMP (2 mM) with or without KT5823 (1 μM) for 10 minutes. Data are given as the mean ± SE (n=6–8 experiments and 8–20 cells per experiment). V4 indicates TRPV4, P2 indicates TRPP2, and $P2^{S827A}$ and $P2^{T719A}$ are point mutants of TRPP2, respectively. $^{\diamond}P<0.01$ compared with vector. $^{\Psi}P<0.01$ compared with 8-Br-cGMP alone. $^{\infty}P<0.01$ compared with V4+P2 without 8-Br-cGMP. $^{\&}P<0.01$ compared with V4+P2 with 8-Br-cGMP.

A and B). In contrast, 8-Br-cGMP markedly reduced the magnitude of flow-induced $[Ca^{2+}]_i$ rises in the cells that were coexpressed with TRPV4 and TRPP2 (Figure 5, C and D). KT5823 (1 μM), a potent and highly specific PKG inhibitor, reversed the inhibitory action of 8-Br-cGMP (Figure 5, C and D). Point mutants were constructed in which two putative PKG phosphorylation sites on TRPP2 (T719A and S827A) were mutated; 8-Br-cGMP inhibition was reduced if TRPP2 was replaced with $TRPP2^{T719A}$ or $TRPP2^{S827A}$ (Figure 5E). cGMP inhibition was abolished if the double mutant $TRPP2^{T719A\text{-}S827A}$ was used to replace TRRP2 (Figure 5E). These data indicate that PKG had no direct effect on TRPV4. Instead, it inhibited the function of heteromeric TRPV4-P2 channels by phosphorylating on the Thr-719 and Ser-827 of TRPP2. Note that cGMP did not have as great an effect on the Ca^{2+} entry in TRPV4-P2–coexpressing HEK293 cells compared with M1-CCD cells. This result could be because of the formation of not only heteromeric TRPV4-P2 but also homomeric TRPV4 when HEK293 cells were cotransfected with TRPV4 and TRPP2. As previously mentioned, homomeric TRPV4 is not sensitive to cGMP or PKG.

Endogenous PKG Phosphorylation Sites in M1-CCD cells

To test whether the Ser-827 and Thr-719 on TRPP2 are endogenous PKG phosphorylation sites important for flow regulation in M1-CCD cells, we synthesized two fusion peptides, transactivator of transcription (TAT)-$TRPP2^{S827}$ and TAT-$TRPP2^{T719}$. TAT-$TRPP2^{S827}$ and TAT-$TRPP2^{T719}$ were synthesized by fusing the two PKG phosphorylation sites in TRPP2 to the membrane translocation signals from HIV-1 tat protein.[24] This fusion allowed for the efficient and abundant intracellular delivery of exogenous substrates for PKG ($TRPP2^{S827}$ and $TRPP2^{T719}$) that compete with endogenous PKG phosphorylation sites, shielding the endogenous PKG phosphorylation sites of TRPP2 from PKG attack. The results show that treating M1-CCD cells with TAT-$TRPP2^{S827}$ (100 nM) or TAT-$TRPP2^{T719}$ (100 nM) markedly reduced the 8-Br-cGMP inhibition on flow-induced $[Ca^{2+}]_i$ rises (Figure 6). The combined application of TAT-$TRPP2^{S827}$+TAT-$TRPP2^{T719}$ abolished the 8-Br-cGMP inhibition on flow-induced $[Ca^{2+}]_i$ rises (Figure 6). These data strongly suggest that cGMP and PKG acted on Ser-827 and Thr-719 of TRPP2 to inhibit heteromeric TRPV4-P2 channels in M1-CCD cells.

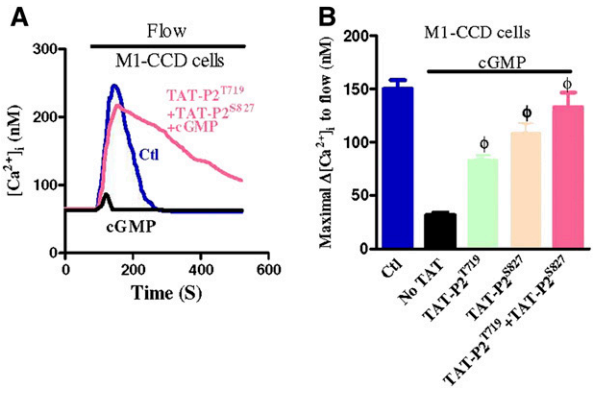

Figure 6. PKG phosphorylation sites in M1-CCD cells. (A) Representative traces illustrating the time course of flow-induced $[Ca^{2+}]_i$ responses. (B) Summary showing the maximal change in flow-induced $[Ca^{2+}]_i$ responses ($\Delta[Ca^{2+}]_i$). All cells were bathed in NPSS containing 1% BSA. Cells were pretreated with 8-Br-cGMP (2 mM) with or without TAT-$P2^{T719}$ (100 nM) and/or TAT-$P2^{S827}$ (100 nM) for 10 minutes before flow. Data are given as the mean ± SE (n=6–8 experiments and 8–20 cells per experiment). $^{\Phi}P<0.01$ versus 8-Br-cGMP.

DISCUSSION

The major findings of this study are as follows. (*1*) Atrial natriuretic peptide, nitric oxide, and cGMP, through their actions on PKG, inhibit flow-induced Ca^{2+} entry in M1-CCD cells. (*2*) Coimmunoprecipitation, double immunostaining, and functional studies suggest that heteromeric TRPV4-P2 channels mediate the flow-induced Ca^{2+} entry in M1-CCD cells and HEK293 cells that are overexpressed with TRPV4 and TRPP2. Together, these data showed the critical role of PKG regulation of heteromeric TRPV4-P2 channels in flow-induced Ca^{2+} entry in M1-CCD cells. Evidence of PKG involvement is strong, including the following findings. First, we observed the 8-Br-cGMP inhibition and the KT5823 reversal of flow-induced Ca^{2+} entry in both M1-CCD cells and HEK293 cells that were coexpressed with TRPV4 and TRPP2. KT5823 is a highly selective inhibitor for PKG, with K_i=0.234 μM.[15] At the concentration that we used (1 μM), it should not affect protein kinase A (K_i>10 μM). However, we could not completely rule out the involvement of protein kinase C (K_i=4 μM).[15] Second, in the HEK293 overexpression system, point mutation at two putative PKG phosphorylation sites on TRPP2 proteins ($TRPP2^{T719A–S827A}$) abolished the inhibitory action of cGMP on flow-induced Ca^{2+} entry. Third, in M1-CCD cells, the application of fusion peptides TAT-$TRPP2^{T719}$+TAT-$TRPP2^{S827}$, which compete with endogenous PKG phosphorylation sites on TRPP2, abolished the inhibitory action of cGMP on flow-induced Ca^{2+} entry. These results support that PKG acts on the Thr-719 and Ser-829 of TRPP2 to inhibit heteromeric TRPV4-P2 channels in M1-CCD cells.

$[Ca^{2+}]_i$ level is an important second messenger that affects K^+ secretion in renal CCD epithelial cells. It is well documented that fluid flow in the renal tubule induces $[Ca^{2+}]_i$ rises in CCD cells, which subsequently stimulate large-conductance Ca^{2+}-activated K^+ channels that result in K^+ secretion in these cells.[2,6] In the present study, we found that atrial natriuretic peptide and nitric oxide, through their action on PKG, inhibited the flow-induced $[Ca^{2+}]_i$ entry in M1-CCD cells. Previously, atrial natriuretic peptide and nitric oxide were known to inhibit Na^+ reabsorption in CCD.[4,5] Because transepithelial Na^+ absorption in the CCD is the major determinant for K^+ secretion,[3] we speculate that atrial natriuretic peptide and nitric oxide, through their actions on PKG, would inhibit Na^+ absorption, which in turn, reduces the K^+ secretion. Additional studies are needed to explore the precise role of this pathway in regulating distal tubular transport.

Several TRP channels have previously been proposed as candidates for mediating the flow-induced Ca^{2+} entry in renal epithelial cells and vascular endothelial cells—two major cell types that are exposed to fluid flow *in vivo*. These candidate channels include TRPV4,[7,8] TRPP1-P2 complex,[9] heteromeric TRPV4-P2,[10] and heteromeric TRPV4-C1.[11] Our coimmunoprecipitation and double immunostaining experiments showed the physical association of TRPV4 and TRPP2. In functional studies, dominant negative mutants of TRPV4 and TRPP2 ($TRPV4^{M680D}$ and $TRPP2^{D511V}$, respectively) each abolished the flow-induced Ca^{2+} entry in M1-CCD cells, indicating an absolute requirement for both TRPV4 and TRPP2 in the flow response. These data suggest that, in renal M1-CCD cells, heteromeric TRPV4-P2 channels are responsible for flow-induced Ca^{2+} entry. As a support, when TRPV4 and TRPP2 were coexpressed in HEK293 cells, they also formed a flow-sensitive Ca^{2+} entry channel, the activity of which was inhibited by $TRPV4^{M680D}$, $TRPP2^{D511V}$, cGMP, and PKG. However, note that the decay kinetics of flow-induced $[Ca^{2+}]_i$ transients were very different between M1-CCD cells and TRPV4-P2–coexpressing HEK293 cells. In M1-CCD cells, the $[Ca^{2+}]_i$ responses were transient (Figure 1A), whereas in HEK293 cells that were coexpressed with TRPV4 and TRPP2, the $[Ca^{2+}]_i$ responses were sustained (Figure 4A). We speculate that the transient nature of the $[Ca^{2+}]_i$ response in M1-CCD cells is, at least partly, because of a Ca^{2+}-mediated negative feedback inhibition on TRPV4-P2 channels. Similar feedback inhibition has been well documented in vascular endothelial cells.[25–27] In this feedback mechanism, Ca^{2+} influx would stimulate a nitric oxide-cGMP-PKG cascade, resulting in a negative feedback inhibition on Ca^{2+} entry channels (*i.e.*, heteromeric TRPV4-P2 channels in this case). The following sets of data support this notion: (*1*) the effect of KT5823 on flow-induced $[Ca^{2+}]_i$ transients in M1-CCD cells (Figure 1A) and (*2*) the effect of TAT-$TRPP2^{T719}$+TAT-$TRPP2^{S827}$ on flow-induced $[Ca^{2+}]_i$ transients in M1-CCD cells (Figure 6A). KT5823 and TAT-$TRPP2^{mutant}$ treatments are both expected to interrupt the feedback loop of nitric oxide-cGMP-PKG-Ca^{2+} entry channels, making the $[Ca^{2+}]_i$ transients more sustained. Our results (Figures 1A and 6A) support the hypothesis. Wild-type HEK293 cells lack the components of nitric oxide-cGMP-PKG signal cascades, leaving them unable to exhibit such a negative feedback inhibition.

As for other potential candidate channels, homomeric TRPV4 and heteromeric TRPV4-C1 channels are unlikely to be involved in M1-CCD cells, because the flow-induced $[Ca^{2+}]_i$ responses have an absolute requirement for TRPP2 based on the effective dominant negative function of $TRPP2^{D511V}$ on the $[Ca^{2+}]_i$ responses. TRPC1 was reported to be expressed only in the proximal tubule and thin descending limb but not in the connecting tubule or the CCD.[28] In our experiments, a TRPC1-specific blocking antibody T1E3 had no effect on the flow-induced Ca^{2+} entry in M1-CCD cells (Figure 2), further supporting that TRPC1 was not involved. Based on the dominant negative effect of $TRPV4^{M680D}$, TRPV4 is also absolutely required for the flow-induced $[Ca^{2+}]_i$ responses in M1-CCD cells. These data argue against the involvement of the TRPP1-P2 complex. However, we cannot exclude the possibility that TRPP1 may interact with heteromeric TRPV4-P2 to mediate flow response. In fact, TRPP1 was reported to be located in the cilia,[9] a crucial structure for flow sensation in renal epithelial cells.[29,30] We found that TRPV4 and TRPP2 are also colocalized in the primary cilia of M1-CCD cells. Additional studies are needed to explore whether TRPP1 could interact

with heteromeric TRPV4-P2 channels in cilia to mediate the flow responses.

In conclusion, the present study shows that flow-induced Ca^{2+} entry in M1-CCD cells is mediated by heteromeric TRPV4-P2 channels and that atrial natriuretic peptide, nitric oxide, and cGMP inhibit the Ca^{2+} influx through PKG-mediated phosphorylation on TRPP2 subunits.

CONCISE METHODS

Cell Culture, Cloning, and Transfection

HEK293 cells were cultured in DMEM supplemented with FBS (10%), penicillin (100 μg/ml), and streptomycin (100 U/ml). The M1-CCD cell line (CRL-2038; American Type Culture Collection, Manassas, VA) is derived from renal CCD microdissected from a mouse transgenic for the early region of the SV40 virus [strain Tg(SV40E) Bri7].[31] M1-CCD cells were cultured in 1:1 DMEM and Ham's F-12 medium with FBS (10%) supplemented with L-glutamine (2 mM), penicillin (100 μg/ml), streptomycin (100 U/ml), and dexamethasone (5 μM). All cells were grown at 37°C in a 5% CO_2 humidified incubator.

The mouse TRPV4 gene (NM_022017) and TRPV4^{M680D} were gifts from Bernd Nilius. TRPP2 was a gift from Gregory Germino. TRPP2^{D511V} was a gift from Rong Ma. TRPP2 point mutations were generated by a QuikChange Site-Directed Mutagenesis Kit (Stratagene). Mutagenic oligonucleotides were CAA ACT AAA ACT GAA AAG AAA CGC TGT AGA TGC CAT CTC AGA GAG for T719A and CCA GAG CC GGA GGG GAG CCA TCT CCA GTG GGG for S827A. All genes were cloned into a pcDNA6 vector for expression. All clones were autosequenced by an ABI310 autosequencer to verify the authenticity of the genes.

HEK293 cells or M1-CCD cells were transfected with various constructs using Lipofectamine 2000 as described elsewhere.[11] Transfection was achieved with 4 μg plasmid DNA from each construct and 6 μl Lipofectamine 2000 in 200 μl Opti-MEM reduced serum medium in six-well plates. About 80% of the HEK293 or M1-CCD cells were successfully transfected by the respective protocols, which was indicated by control transfection using a GFP-expressing pCAGGS vector or GFP-tagged TRPV4 and GFP-tagged TRPP2. A stable PKG-containing cell line was established under the selection pressure of blasticidin. Functional studies were performed 2–3 days post-transfection.

Fluorescent Immunostaining of Cultured Cells

A double immunofluorescence assay was performed. Briefly, M1-CCD or HEK293 cells coexpressing TRPV4 and -P2 were seeded on glass coverslips. The cells were rinsed with PBS three times, fixed with 3.7% paraformaldehyde, and permeabilized with 0.2% Triton X-100. Nonspecific immunostaining was blocked by incubating the cells with 2% BSA in PBS. The cells were then incubated with anti-TRPV4 (rabbit polyclonal antibody; Alomone Labs) for 1 hour at room temperature. After three washes with PBS, the cells were incubated with an anti-TRPP2 (G20, goat polyclonal antibody; Santa Cruz Biotechnology) antibody for 1 hour at room temperature. After three washes with PBS, the cells were incubated for 1 h with the following pairs of secondary antibodies: donkey anti-rabbit IgG conjugated to Alexa Fluor 488 (1:200) and donkey anti-goat IgG conjugated to Alexa Fluor 546 (1:100). After washing and mounting, immunofluorescence of the cells was detected using an FV1000 confocal system.

Coimmunoprecipitation and Immunoblots

Coimmunoprecipitation and immunoblots were as described elsewhere.[11] In brief, whole-cell lysates from M1-CCD cells or HEK293 cells overexpressing TRPV4 and -P2 were extracted with a detergent extraction buffer containing 1% (vol/vol) Nonidet P-40, 150 mM NaCl, and 20 mM Tris·HCl (pH 8.0) along with protease inhibitor cocktail tablets. TRPV4 or TRPP2 proteins were immunoprecipitated by incubating 800 μg extracted proteins with 5 μg anti-TRPP2 (G20; Santa Cruz Biotechnology) or anti-TRPV4 (Alomone Lab) antibody on a rocking platform overnight at 4°C. Protein A agarose (for TRPV4 antibody) or protein G agarose (for TRPP2 antibody) was then added and incubated for an additional 3 hours at 4°C. The immunoprecipitates were washed three times with PBS.

For the immunoblots, all of the samples were fractionated by 7.5% SDS-PAGE, transferred to poly(vinylidene difluoride) membranes, and probed with the indicated primary antibodies at 1:200 dilution in a phosphate-buffered saline with Tween-20 buffer that contained 0.1% Tween-20 and 5% nonfat dry milk. Immunodetection was accomplished using horseradish peroxidase-conjugated secondary antibody followed by an enhanced chemiluminescence detection system.

Preparation of T1E3 and Preimmune IgG

The T1E3 antibody was raised in rabbits using the strategy described.[19,32] Briefly, a peptide corresponding to the TRPC1 putative pore region (CVGIFCEQQSNDTFHSFIGT) was synthesized and conjugated to a keyhole limpet hemocyanin at Alpha Diagnostic International. The coupled T1E3 peptide was injected to the back of a rabbit followed by two boost doses. T1E3 antiserum was collected 4 weeks after the second boost. IgG was purified from the T1E3 antiserum and the preimmune serum using a protein G column.

$[Ca^{2+}]_i$ Measurement

Cell preparation and Ca^{2+} measurements were performed as described.[11] Cells were loaded with Furo-2-AM and pluronic F127 in a normal physiologic solution (NPSS) containing 140 mM NaCl, 5 mM KCl, 1 mM $CaCl_2$, 1 mM $MgCl_2$, 10 mM glucose, and 5 mM Hepes (pH 7.4). Flow was initiated by pumping NPSS containing 1% BSA into a specially designed parallel plate flow chamber that resembled the one described in the work by Kanai *et al.*,[33] in which the cells adhered to the bottom. Shear stress was ~5 dyne/cm^2 and in some experiments, 0.5 dyne/cm^2. In experiments assessing the flow response in Ca^{2+}-free condition, the cells were exposed to Ca^{2+}-free solution for less than 2 minutes to the avoid undesirable effect of Ca^{2+} store depletion. The Ca^{2+}-bound and -unbound Fura-2 fluorescence signals were measured using dual excitation wavelengths at 340 and 380 nm using an Olympus fluorescence imaging system. Fura-2 ratio change was then converted to $[Ca^{2+}]_i$. The conversion was based on a standard curve that was constructed using commercially available Ca^{2+} standard solutions of different concentrations. The fluorescence in

an area without cells was taken as background and subtracted; 10–20 cells were analyzed in each experiment. Experiments were performed at room temperature.

TAT-Mediated Protein Transduction into M1-CCD Cells

Small peptides that contain TRPP2 PKG phosphorylation sites (TRPP2^{S827}, SRRRGSIS; TRPP2^{T719}, KLKRNTVD) were conjugated to an NH_2-terminal 11-amino acid HIV tat protein transduction domain (YGRKKRRQRRR) at Alpha Diagnostic International.[24] M1-CCD cells were pretreated with TAT-TRPP2^{S827} (100 nM) and/or TAT-TRPP2^{T719} (100 nM) at room temperature for at least 10 minutes before Ca^{2+} measurement.

Materials

Fura-2/AM and Pluronic F-127 were obtained from Molecular Probes. DMEM, DMEM/F12, PBS, Opti-MEM, FBS, Lipofectamine 2000, and protease inhibitors were from Invitrogen. Anti-TRPV4 antibodies were from Alomone Laboratories. Anti-TRPP2 antibody (G20) was from Santa Cruz Biotechnology. Nonidet P-40, sodium deoxycholate, SDS, $CaCl_2$, BSA, glucose, Tris·HCl, trypsin, and $MgCl_2$ were purchased from Sigma.

Statistical Analyses

A *t* test was used for statistical comparison. For the comparison of multiple groups, one-way ANOVA with Newman–Keuls was used. Significances were set as $P<0.05$.

ACKNOWLEDGMENTS

This work was supported by Hong Kong Research Grants Council Grants CUHK478011, CUHK479109, and CUHK478710, Strategic Investment Scheme C, a Group Research Grant from the Chinese University of Hong Kong, and National Science Foundation of China Grant 30800384.

DISCLOSURES

None.

REFERENCES

1. Giebisch G: Renal potassium transport: Mechanisms and regulation. *Am J Physiol* 274: F817–F833, 1998
2. Liu W, Morimoto T, Woda C, Kleyman TR, Satlin LM: Ca2+ dependence of flow-stimulated K secretion in the mammalian cortical collecting duct. *Am J Physiol Renal Physiol* 293: F227–F235, 2007
3. Satlin LM, Sheng S, Woda CB, Kleyman TR: Epithelial Na(+) channels are regulated by flow. *Am J Physiol Renal Physiol* 280: F1010–F1018, 2001
4. Zeidel ML: Renal actions of atrial natriuretic peptide: Regulation of collecting duct sodium and water transport. *Annu Rev Physiol* 52: 747–759, 1990
5. Ortiz PA, Garvin JL: Role of nitric oxide in the regulation of nephron transport. *Am J Physiol Renal Physiol* 282: F777–F784, 2002
6. Satlin LM, Carattino MD, Liu W, Kleyman TR: Regulation of cation transport in the distal nephron by mechanical forces. *Am J Physiol Renal Physiol* 291: F923–F931, 2006
7. Wu L, Gao X, Brown RC, Heller S, O'Neil RG: Dual role of the TRPV4 channel as a sensor of flow and osmolality in renal epithelial cells. *Am J Physiol Renal Physiol* 293: F1699–F1713, 2007
8. Taniguchi J, Tsuruoka S, Mizuno A, Sato J, Fujimura A, Suzuki M: TRPV4 as a flow sensor in flow-dependent K^+ secretion from the cortical collecting duct. *Am J Physiol Renal Physiol* 292: F667–F673, 2007
9. Nauli SM, Alenghat FJ, Luo Y, Williams E, Vassilev P, Li X, Elia AEH, Lu W, Brown EM, Quinn SJ, Ingber DE, Zhou J: Polycystins 1 and 2 mediate mechanosensation in the primary cilium of kidney cells. *Nat Genet* 33: 129–137, 2003
10. Köttgen M, Buchholz B, Garcia-Gonzalez MA, Kotsis F, Fu X, Doerken M, Boehlke C, Steffl D, Tauber R, Wegierski T, Nitschke R, Suzuki M, Kramer-Zucker A, Germino GG, Watnick T, Prenen J, Nilius B, Kuehn EW, Walz G: TRPP2 and TRPV4 form a polymodal sensory channel complex. *J Cell Biol* 182: 437–447, 2008
11. Ma X, Qiu S, Luo J, Ma Y, Ngai CY, Shen B, Wong CO, Huang Y, Yao X: Functional role of vanilloid transient receptor potential 4-canonical transient receptor potential 1 complex in flow-induced Ca2+ influx. *Arterioscler Thromb Vasc Biol* 30: 851–858, 2010
12. Everaerts W, Nilius B, Owsianik G: The vanilloid transient receptor potential channel TRPV4: From structure to disease. *Prog Biophys Mol Biol* 103: 2–17, 2010
13. Andrade YN, Fernandes J, Vázquez E, Fernández-Fernández JM, Arniges M, Sánchez TM, Villalón M, Valverde MA: TRPV4 channel is involved in the coupling of fluid viscosity changes to epithelial ciliary activity. *J Cell Biol* 168: 869–874, 2005
14. Tsiokas L: Function and regulation of TRPP2 at the plasma membrane. *Am J Physiol Renal Physiol* 297: F1–F9, 2009
15. Gadbois DM, Crissman HA, Tobey RA, Bradbury EM: Multiple kinase arrest points in the G1 phase of nontransformed mammalian cells are absent in transformed cells. *Proc Natl Acad Sci USA* 89: 8626–8630, 1992
16. Weinbaum S, Duan Y, Satlin LM, Wang T, Weinstein AM: Mechanotransduction in the renal tubule. *Am J Physiol Renal Physiol* 299: F1220–F1236, 2010
17. Voets T, Prenen J, Vriens J, Watanabe H, Janssens A, Wissenbach U, Bödding M, Droogmans G, Nilius B: Molecular determinants of permeation through the cation channel TRPV4. *J Biol Chem* 277: 33704–33710, 2002
18. Ma R, Li WP, Rundle D, Kong J, Akbarali HI, Tsiokas L: PKD2 functions as an epidermal growth factor-activated plasma membrane channel. *Mol Cell Biol* 25: 8285–8298, 2005
19. Kwan HY, Shen B, Ma X, Kwok YC, Huang Y, Man YB, Yu S, Yao X: TRPC1 associates with $BK_{(Ca)}$ channel to form a signal complex in vascular smooth muscle cells. *Circ Res* 104: 670–678, 2009
20. Xu SZ, Beech DJ: TrpC1 is a membrane-spanning subunit of store-operated $Ca^{(2+)}$ channels in native vascular smooth muscle cells. *Circ Res* 88: 84–87, 2001
21. Yang XR, Lin MJ, McIntosh LS, Sham JS: Functional expression of transient receptor potential melastatin- and vanilloid-related channels in pulmonary arterial and aortic smooth muscle. *Am J Physiol Lung Cell Mol Physiol* 290: L1267–L1276, 2006
22. Bai CX, Kim S, Li WP, Streets AJ, Ong AC, Tsiokas L: Activation of TRPP2 through mDia1-dependent voltage gating. *EMBO J* 27: 1345–1356, 2008
23. Kwan HY, Huang Y, Yao X: Regulation of canonical transient receptor potential isoform 3 (TRPC3) channel by protein kinase G. *Proc Natl Acad Sci USA* 101: 2625–2630, 2004
24. Schwarze SR, Ho A, Vocero-Akbani A, Dowdy SF: In vivo protein transduction: delivery of a biologically active protein into the mouse. *Science* 285: 1569–1572, 1999
25. Yao X, Huang Y: From nitric oxide to endothelial cytosolic Ca^{2+}: A negative feedback control. *Trends Pharmacol Sci* 24: 263–266, 2003

26. Yao X, Kwan HY, Chan FL, Chan NW, Huang Y: A protein kinase G-sensitive channel mediates flow-induced Ca($^{2+}$) entry into vascular endothelial cells. *FASEB J* 14: 932–938, 2000
27. Kwan HY, Leung PC, Huang Y, Yao X: Depletion of intracellular Ca^{2+} stores sensitizes the flow-induced Ca^{2+} influx in rat endothelial cells. *Circ Res* 92: 286–292, 2003
28. Goel M, Sinkins WG, Zuo CD, Estacion M, Schilling WP: Identification and localization of TRPC channels in the rat kidney. *Am J Physiol Renal Physiol* 290: F1241–F1252, 2006
29. Schwartz EA, Leonard ML, Bizios R, Bowser SS: Analysis and modeling of the primary cilium bending response to fluid shear. *Am J Physiol* 272: F132–F138, 1997
30. Liu W, Xu S, Woda C, Kim P, Weinbaum S, Satlin LM: Effect of flow and stretch on the $[Ca^{2+}]_i$ response of principal and intercalated cells in cortical collecting duct. *Am J Physiol Renal Physiol* 285: F998–F1012, 2003
31. Stoos BA, Náray-Fejes-Tóth A, Carretero OA, Ito S, Fejes-Tóth G: Characterization of a mouse cortical collecting duct cell line. *Kidney Int* 39: 1168–1175, 1991
32. Xu SZ, Zeng F, Lei M, Li J, Gao B, Xiong C, Sivaprasadarao A, Beech DJ: Generation of functional ion-channel tools by E3 targeting. *Nat Biotechnol* 23: 1289–1293, 2005
33. Kanai AJ, Strauss HC, Truskey GA, Crews AL, Grunfeld S, Malinski T: Shear stress induces ATP-independent transient nitric oxide release from vascular endothelial cells, measured directly with a porphyrinic microsensor. *Circ Res* 77: 284–293, 1995

This article contains supplemental material online at http://jasn.asnjournals.org/lookup/suppl/doi:10.1681/ASN.2011100972/-/DCSupplemental.